Application Note

Biopharma

Agilent

Trusted Answers

HILIC Analysis of CRISPR-Cas9 Gene Editing Tools on a Low Adsorption LC Flow Path

Using the Agilent 1290 Infinity III Bio LC System and Ultra-Inert Column Hardware

Authors

Helena Vanluchene,
Jelle De Vos, Kris Morreel,
Pat Sandra, and Koen Sandra
RIC group,
President Kennedypark 6,
8500 Kortrijk, Belgium

Sonja Schneider and
Udo Huber
Agilent Technologies, Inc.

Abstract

Five years ago, the first mRNA-based medicines were introduced to the market at an unprecedented speed. Their pivotal role across diverse therapeutic areas underscores the urgent need for advanced analytical methodologies to enable thorough characterization. HILIC has emerged as a viable and sustainable alternative to traditional IP-RPLC methods for oligonucleotide separation. However, the highly anionic nature of oligonucleotides can lead to adsorption to the iron surfaces of the LC flow path, particularly under HILIC conditions, which adversely affects analyte recovery and peak shape. In this application note, the performance of a traditional stainless-steel HILIC column is compared with that of a deactivated stainless-steel HILIC column for the analysis of sgRNA and Cas9 mRNA digests.

Introduction

The year 2020 marked the breakthrough of the messenger ribonucleic acid (mRNA) technology with the rapid development and global deployment of mRNA vaccines for COVID-19. Their success demonstrated the efficacy, safety, and scalability of the platform, accelerating the development of other mRNA-based medicines. Beyond vaccines, mRNA has since gained growing interest in diverse applications such as cancer immunotherapy, protein replacement, and gene editing.[1] In gene editing, mRNA can play a pivotal role by enabling transient and targeted delivery of the most widely used gene editing enzyme, CRISPR-associated protein 9 (Cas9). Cas9 encoded by mRNA can be readily combined with single guide RNA (sgRNA), which flags the genome site that must be edited, within a single lipid nanoparticle.

Concomitantly, the rapid development of mRNA requires analytical tools to characterize critical quality attributes such as sequence, capping efficiency, poly(A) tail length, modifications, and sequence variants. All these attributes can be comprehensively analyzed by liquid chromatography coupled with mass spectrometry (LC/MS) in an approach known as RNA mapping.[2] This involves the enzymatic digestion of RNA by ribonucleases (RNases) followed by LC/MS analysis of the oligonucleotide mixture. Currently, ion pairing-reversed phase LC (IP-RPLC) is the gold standard for oligonucleotide separation. However, hydrophilic interaction liquid chromatography (HILIC) is gaining interest for oligonucleotide separations as a cleaner, more sustainable alternative that provides complementary selectivity to IP-RPLC.[3-5]

HILIC separation relies primarily on the partitioning of oligonucleotides between an apolar mobile phase, typically composed of acetonitrile, and a water-layered polar stationary phase. Other interactions such as adsorptive interactions (e.g. hydrogen bonding) and electrostatic interactions between the oligonucleotides and the stationary phase contribute to the overall retention process.[6] Despite specific advantages of HILIC over IP-RPLC for oligonucleotide separations, this technique faces its own challenges, including lower MS sensitivity and the nonspecific adsorption of oligonucleotides to metal surfaces in the LC flow path (tubing, needle, column housing, and frit), which can compromise recovery, reproducibility, and peak shape.

Oligonucleotides are highly negatively charged due to the presence of phosphate moieties, making them particularly susceptible to adsorption on stainless-steel surfaces. Indeed, the phosphate groups of oligonucleotides tend to adsorb to the positively charged thin metal oxide layer on stainless-steel surfaces and can stick to leached metal-ions retained by the stationary phase. In a workaround, metal chelators, such as ethylenediaminetetraacetic acid (EDTA) or medronic acid, can be added to the mobile phase to circumvent adsorption to leached metal ions. At the same time, adsorption to the stainless-steel surface should be minimized, which can be achieved by adding citrate or phosphate to the mobile phase, or by repetitive injection of oligonucleotides to passivate the column. However, mobile phase additives are not a preferred choice since they might result in a lower MS response. Column passivation can be considered a mitigation strategy, but it does not guarantee a long-lasting solution and complete coverage of all active sites on the stainless-steel surface, as the effect may diminish over time and some active sites may remain accessible to analytes. As an alternative, LC hardware can be manufactured from materials other than stainless steel, such as nickel cobalt MP35N alloy or polyether ether ketone (PEEK). Stainless-steel surfaces in columns can also be deactivated by application of an inert coating in column production. PEEK-lined columns have shown potential for oligonucleotide separations, but come with inherent limitations. Compared to conventional stainless-steel columns, the production of PEEK-lined columns with consistent internal diameter is challenging, and special attention should be given to the connectors used to install the column. Additionally, PEEK is incompatible with certain solvents, and its hydrophobic nature can cause undesired secondary interactions with hydrophobic analytes. MP35N, on the other hand, can leach nickel and cobalt. This application note focuses on the HILIC-based separation of oligonucleotides originating from sgRNA and Cas9 mRNA digest using either a conventional stainless-steel zwitterionic HILIC (HILIC-Z) column or its deactivated alternative using a biocompatible Agilent 1290 Infinity III Bio LC System. The impact of linearizing or removing the 3' phosphate residue is further studied.

Experimental

Materials

Ammonium acetate (LC/MS grade) was obtained from Merck. Type I water was produced using an Arium pro ultrapure lab water system (Sartorius). Acetonitrile (HPLC-S grade) was supplied by Biosolve. The Agilent RNA resolution standard (part number 5190-9028) was provided by Agilent. The endoribonucleases, RNase T1 and RNase 4, and 1x NEBuffer r1.1 were acquired from New England Biolabs. DEPC-treated water was obtained from Thermo Fisher Scientific. Tris(hydroxymethyl)aminomethane (Tris) pH 7.5 buffer and ethylenediaminetetraacetic acid (EDTA) were obtained from Sigma-Aldrich. The enzymes, 2',3'-cyclic-nucleotide 3'-phosphodiesterase (CNP) and calf intestinal alkaline phosphatase (CIP), were acquired from Sanbio and New England Biolabs, respectively. The 50 nucleotide (nt) RNA sample and sgRNA of 104 nt in length were designed in-house and produced by Integrated DNA Technologies. CleanCap Cas9 mRNA (4522 nt) was obtained from TriLink BioTechnologies.

Sample preparation

The RNA resolution standard was dissolved in 1 mL of DEPC-treated water. RNA samples (50 nt RNA, sgRNA, Cas9 mRNA) were enzymatically digested using either RNase T1 or RNase 4. To generate the RNase T1 digests, 5 units of RNase T1 per microgram of sgRNA and 50 units of RNase T1 per microgram of Cas9 mRNA were incubated in a Tris buffer containing EDTA at 37 °C for 30 minutes. For RNase 4 digestion of 50 nt RNA, 0.5 units of RNase 4 per microgram of RNA were added in 1x NEBuffer r1.1 and incubated at 37 °C for one hour. Subsequent treatment of the RNase T1 and 4 digests with CNP involved adding 2 ng of CNP per microgram of RNA and incubating at 37 °C for one hour. Further CIP treatment was performed by adding 0.085 units of CIP per microgram of RNA into the digestion mixture and incubating for one hour at 37 °C.

Instrumentation

Samples were run on an Agilent 1290 Infinity III Bio LC System consisting of an Agilent 1290 Infinity III Bio High-Speed Pump (G7132A), an Agilent 1290 Infinity III Bio Multisampler (G7137A) with integrated sample thermostat, an Agilent 1290 Infinity III Multicolumn Thermostat (G7116B) with Agilent InfinityLab Quick Connect Heat Exchanger 1290 Bio Standard Flow (G711660071), and an Agilent 1290 Infinity III DAD (G7117B) with Agilent InfinityLab Max-Light Cartridge Cell, 10 mm (G4212-60008). Method parameters are summarized in Table 1. Data were acquired and processed in Agilent OpenLab CDS, version 2.7.

Table 1. LC method parameters.

Parameter	Value
Columns	– Agilent InfinityLab Poroshell HILIC-Z, 2.1 × 150 mm, 2.7 µm (p/n 683775-924) – Agilent Altura Poroshell HILIC-Z with Ultra Inert technology, 2.1 × 150 mm, 2.7 µm (p/n 227215-924)
Flow Rate	0.35 mL/min
Mobile Phase	A) 20 mM ammonium acetate in water:acetonitrile 20:80 (v/v) B) 20 mM ammonium acetate in water:acetonitrile 80:20 (v/v)
Gradient (LC Method 1) (RNA Resolution Standard and sgRNA)	Time (min) %B 0 10 17 55 20 90 23 90 25 10 40 10
Gradient (LC Method 2) (Cas9 mRNA)	Time (min) %B 0 10 60 65 63 90 66 90 68 10 85 10
Injection	1 µL
Needle Wash	Flush port, 3s, water:acetonitrile 75:25 (v/v)
Autosampler Temperature	8 °C
Column Temperature	40 °C
Detection DAD	260/4 nm, reference 360/40 nm Peak width > 0.013 min (20 Hz)

Results and discussion

Oligonucleotides are prone to adsorption onto the stainless-steel surfaces of LC hardware, resulting in lower recovery and pronounced peak tailing.[3-6] To evaluate this phenomenon, we compared the extent of oligonucleotide adsorption on a conventional stainless-steel HILIC-Z column and its deactivated counterpart. Before the first sample injection, both columns were equilibrated with 80 column volumes of initial mobile phase to allow the formation of an aqueous layer on the surface of the stationary phase. As illustrated in Figure 1, using repetitive injections of the Agilent RNA resolution standard, composed of four oligonucleotides (14-, 17-, 20-, and 21-mers), metal adsorption was assessed. On the stainless-steel HILIC-Z column (Figure 1A), 25 injections were required to stabilize the UV response and effectively passivate the column, corresponding to the injection of 250 pmol RNA. In contrast, the deactivated column exhibited an immediately stable UV response upon the first injection, suggesting minimal to no adsorption of oligonucleotides to the LC column (Figure 1B). However, even after column conditioning, the stainless-steel HILIC-Z column still exhibited lower peak height and peak area, as well as more pronounced peak tailing, compared to the deactivated column. Additionally, it should be noted that the stainless-steel HILIC-Z column requires reconditioning after storage and before use, indicating that the passivation effect is only temporary.

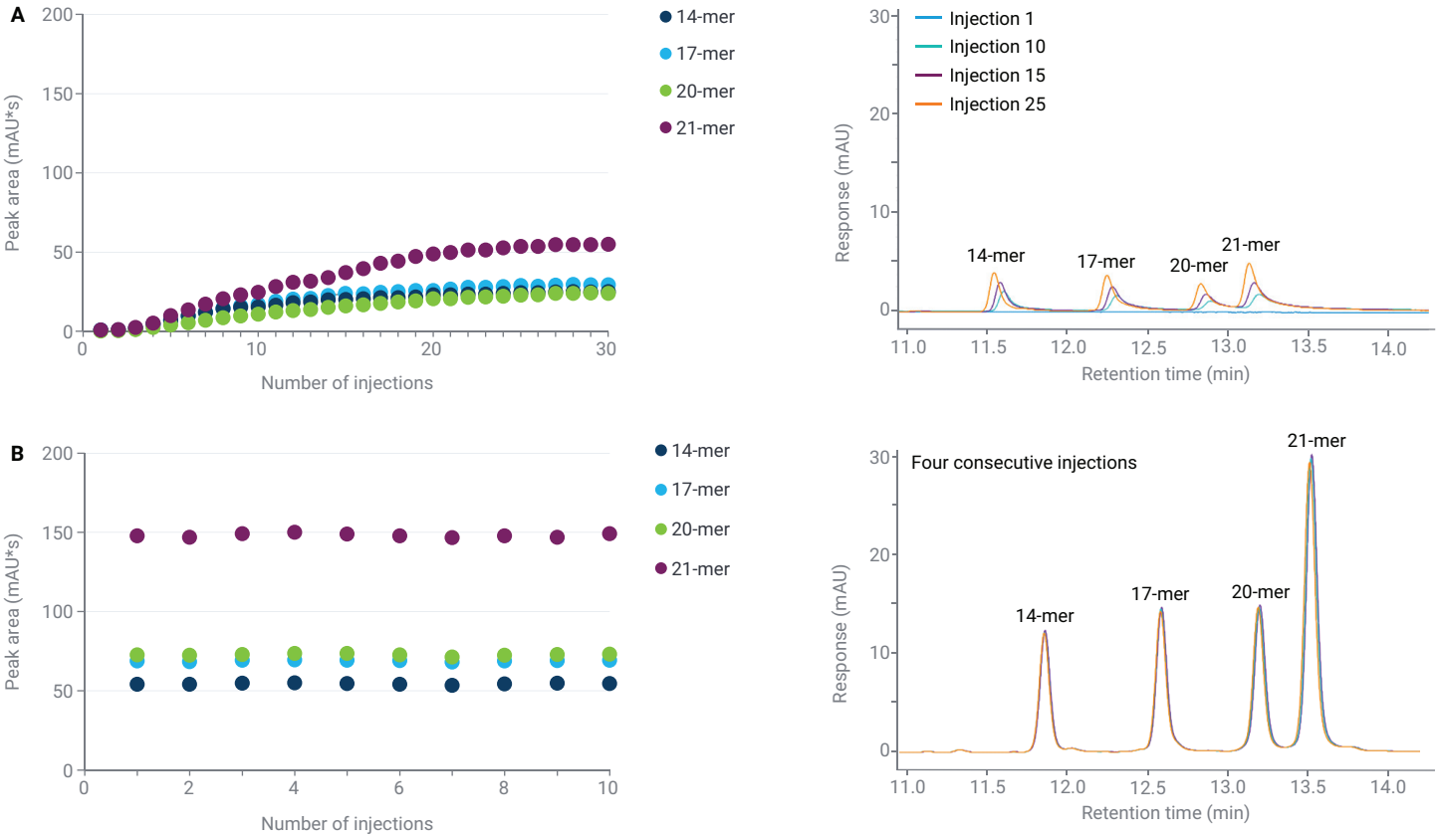

Figure 1. HILIC-UV chromatograms (260 nm) of repeated RNA resolution standard injections on a new conventional stainless-steel (A) and a new deactivated stainless-steel HILIC-Z column (B).

High-quality oligonucleotide separation plays a critical role in RNA mapping. Limited peak capacity in LC results in co-elution, which in turn can overload the MS, leading to convoluted and unreadable spectra.[2] Recently, HILIC has gained increasing attention as a powerful tool for oligonucleotide separation in the context of RNA mapping.[7,8] Prior to LC separation, the RNA is enzymatically digested using RNases. In this application note, the endoribonucleases RNase T1 and RNase 4 were selected for digestion. RNase T1 cleaves single-stranded RNA (ssRNA) specifically at the 3'-end of guanosine (G) residues, whereas RNase 4 cleaves ssRNA at the 3'-end of uridine (U) in uridine-purine sequences (U/A and U/G). The digestion products of RNase T1 and RNase 4 consist of a mixture of 2',3'-cyclic-phoshophorylated and 3'-phosphorylated species (Figure 2), but their relative abundances differ. The hydrolysis step of the 2',3'-cyclic intermediate to the 3'-phosphorylated form proceeds considerably faster with RNase T1 than with RNase 4. Consequently, RNase T1 digestion yields predominantly linear 3'-phosphorylated species, whereas RNase 4 produces an approximately equal mixture of oligonucleotides with cyclic and linear phosphate termini on the oligonucleotides.[7,9] To simplify the digestion mixture, additional enzymatic treatments can be considered after RNase digestion. For example, CNP, which converts 2',3'-cylic phosphate termini into linear 3'-phosphate termini, can be applied. Additionally, CIP can be used to remove linear phosphate groups, generating 3'-hydroxyl ends. Here, these enzymes were applied to get a deeper understanding of the nonspecific adsorption of oligonucleotides to stainless-steel surfaces.

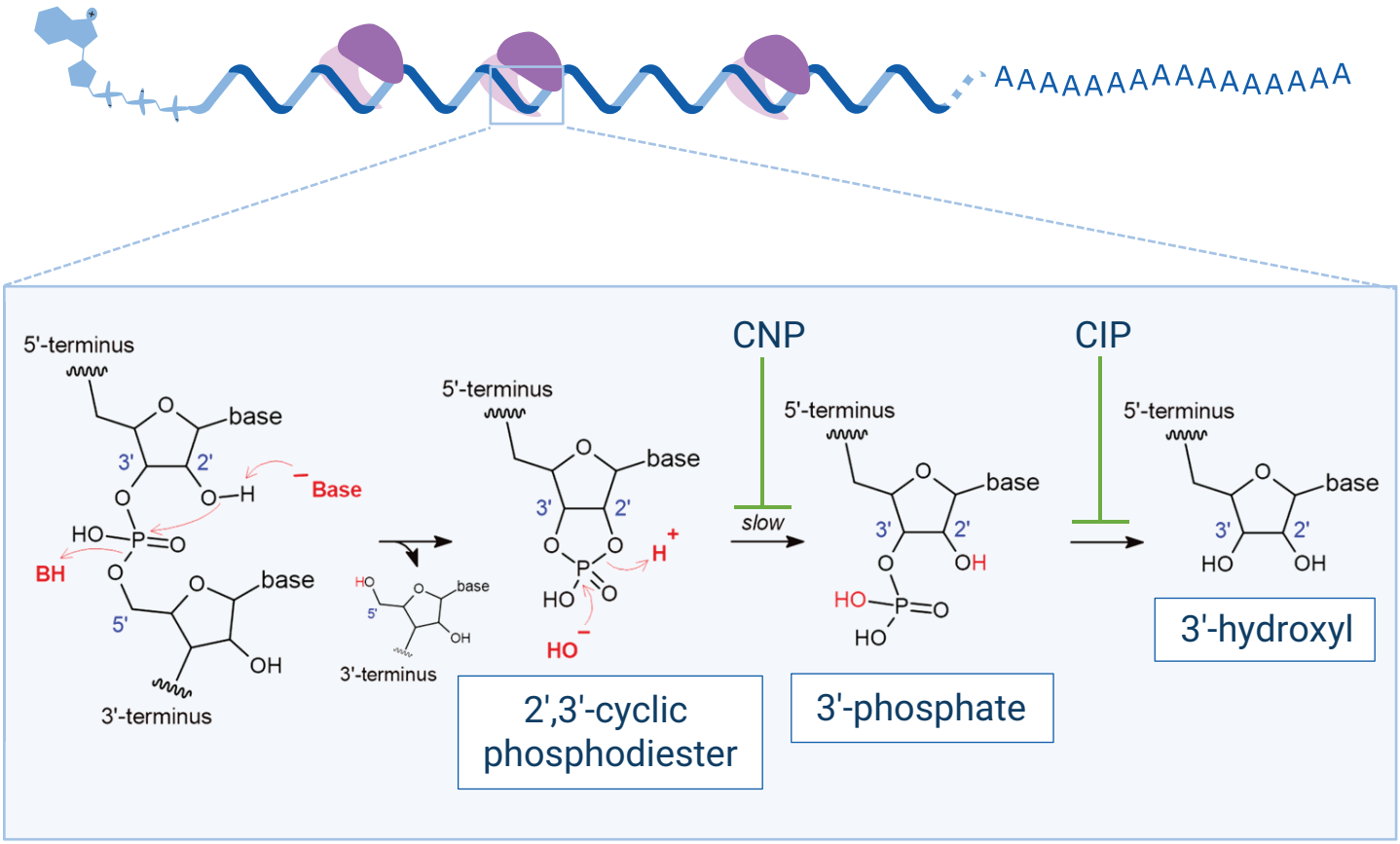

Figure 2. Reaction mechanisms of RNase T1, RNase 4, CNP, and CIP. mRNA is digested by RNase T1 or RNase 4, thereby generating first oligonucleotides with 2'3'-cyclic phosphate termini, which can further be hydrolyzed (slow) to 3'-phospate termini. CNP catalyzes this hydrolysis reaction. CIP hydrolyzes the linear phosphate termini to 3'-hydroxyl termini.

As a simplified model, a custom-designed 50 nt RNA was digested with RNase 4, with or without subsequent treatment with CNP and CIP. The resulting digests were subjected to HILIC-UV on both the fully passivated conventional and the deactivated stainless-steel HILIC-Z column (Figure 3). Both the RNase 4 digest and the RNase 4-CNP-CIP digest display comparable chromatographic profiles on both columns, with slightly increased peak tailing observed on the stainless-steel column. In sharp contrast, the RNase 4-CNP digest, containing only oligonucleotide fragments with a linear 3'-phosphate terminus, exhibited significant chromatographic differences on the two columns. On the fully passivated conventional stainless-steel HILIC-Z column, the digest showed substantially increased peak tailing and reduced peak intensity, illustrative of oligonucleotide adsorption to the residual active sites on the stainless-steel surfaces. In comparison, the deactivated HILIC-Z column produced sharper peaks and higher intensities due to significantly reduced nonspecific adsorption.

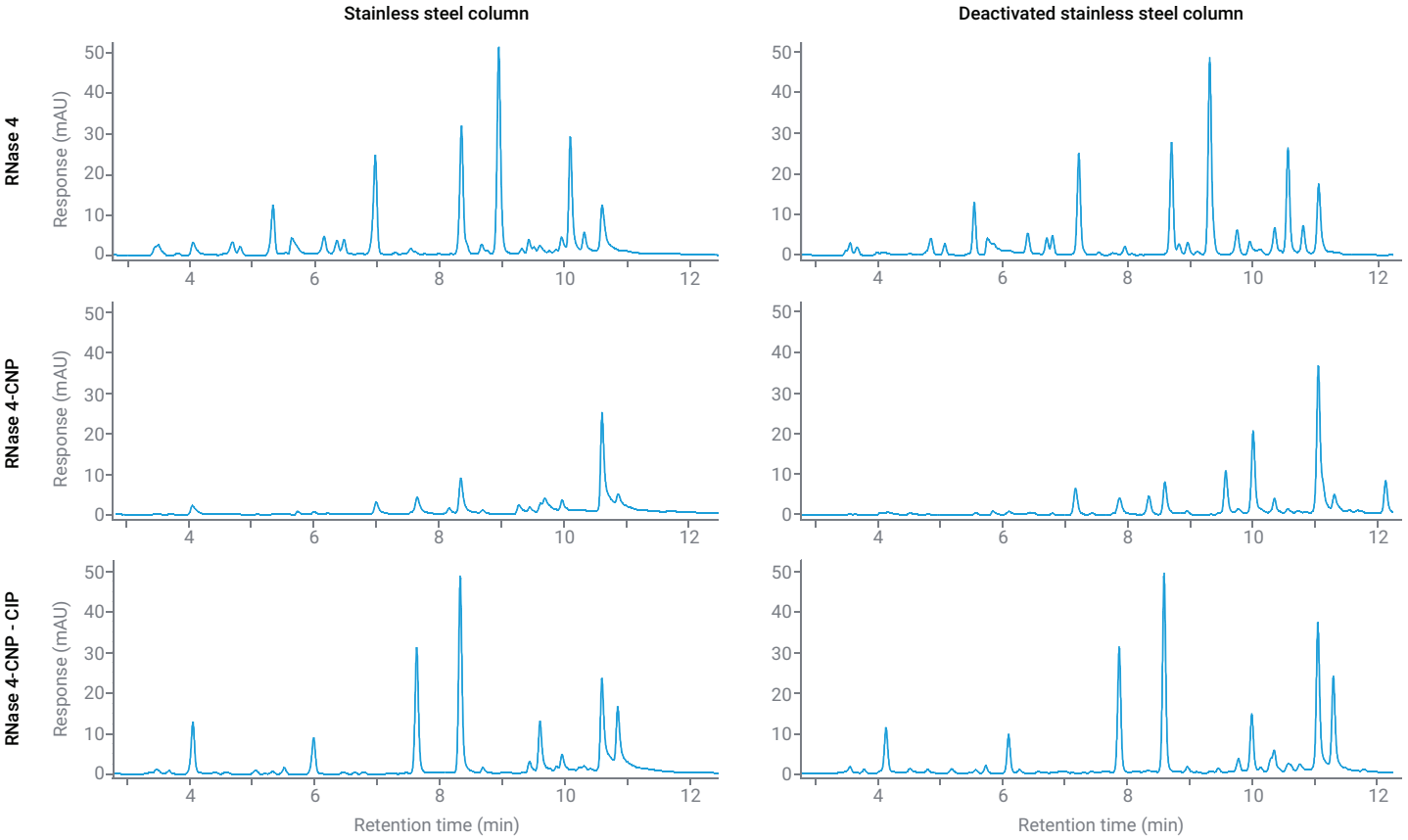

Figure 3. HILIC-UV chromatograms (260 nm) of a 50 nt RNA digested with RNase 4, followed by CNP and CIP treatment, and injected on a fully passivated conventional and deactivated stainless-steel HILIC-Z column (LC Method 1).

A similar set-up was evaluated for two more therapeutically relevant species, including sgRNA and Cas9 mRNA. Both molecules were subjected to digestion by RNase T1, after which a portion of the sample underwent additional enzymatic treatment with CNP and CIP. All samples were injected on both the fully passivated conventional stainless-steel HILIC-Z column and the deactivated column (Figures 4 and 5). For both sgRNA and Cas9 mRNA, it is noted that the chromatograms of the RNase T1 and the RNase T1-CNP digest are essentially identical when analyzed on the same column. This could be attributed to the fact that RNase T1 mainly generates RNA fragments with linear 3'-phosphate groups. Consequently, further treatment with CNP does not significantly alter the digestion mixture based on the HILIC-UV chromatograms. However, a minority of the fragments may have a 2',3'-cyclic phosphate terminus that is susceptible to hydrolysis by CNP, but detection of these low abundant species requires more sensitive techniques, such as MS. On the passivated conventional stainless-steel column, the RNase T1 and RNase T1-CNP digests show pronounced peak tailing and low peak intensities compared to the deactivated stainless-steel column, indicating significant nonspecific adsorption of oligonucleotides to the stainless-steel column surface. However, subsequent treatment with CIP to remove linear 3'-phosphate termini markedly enhanced chromatographic performance on the stainless-steel column, with reduced peak tailing and increased peak intensities. Interestingly, following CIP treatment, HILIC-UV chromatograms were comparable on both columns, although peak shapes and intensities remained slightly better on the deactivated column, suggesting that limited oligonucleotide adsorption to the stainless-steel column persists despite removal of linear 3'-phosphate termini. Overall, our results highlight that oligonucleotide adsorption to stainless-steel is influenced by the nature of the terminal phosphate group. Fragments terminating with linear phosphate groups show significant adsorption, whereas those with cyclic phosphate termini or hydroxyl groups show less interaction. Additionally, it is important to note that nucleotides are linked together by phosphodiester bonds in the oligonucleotide chain, which also contributes to adsorption to a certain extent.

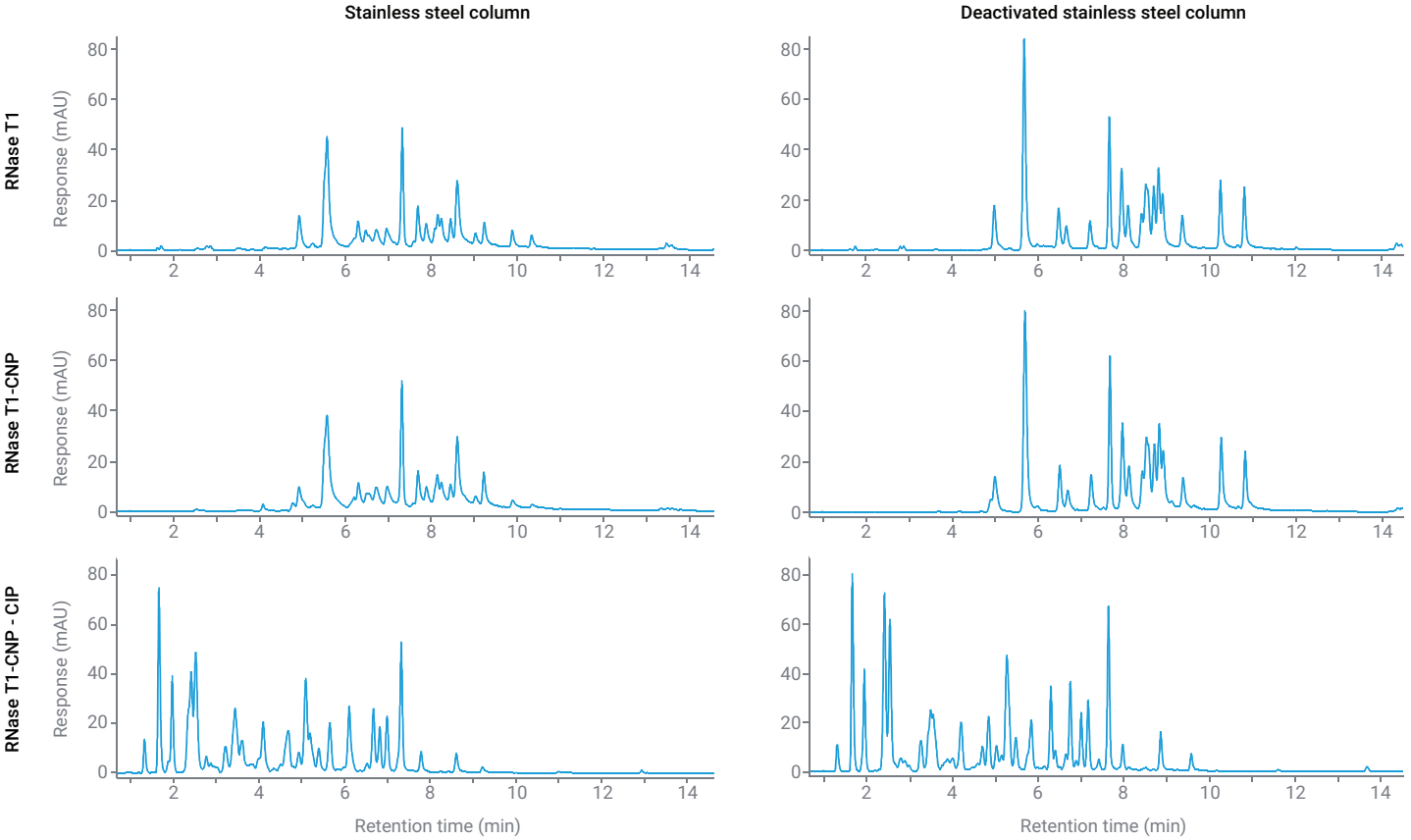

Figure 4. HILIC-UV chromatograms (260 nm) of a sgRNA digested with RNase T1, sequentially treated with CNP and CIP, and analyzed on both a fully passivated conventional stainless-steel HILIC-Z column and a deactivated HILIC-Z column (LC Method 1).

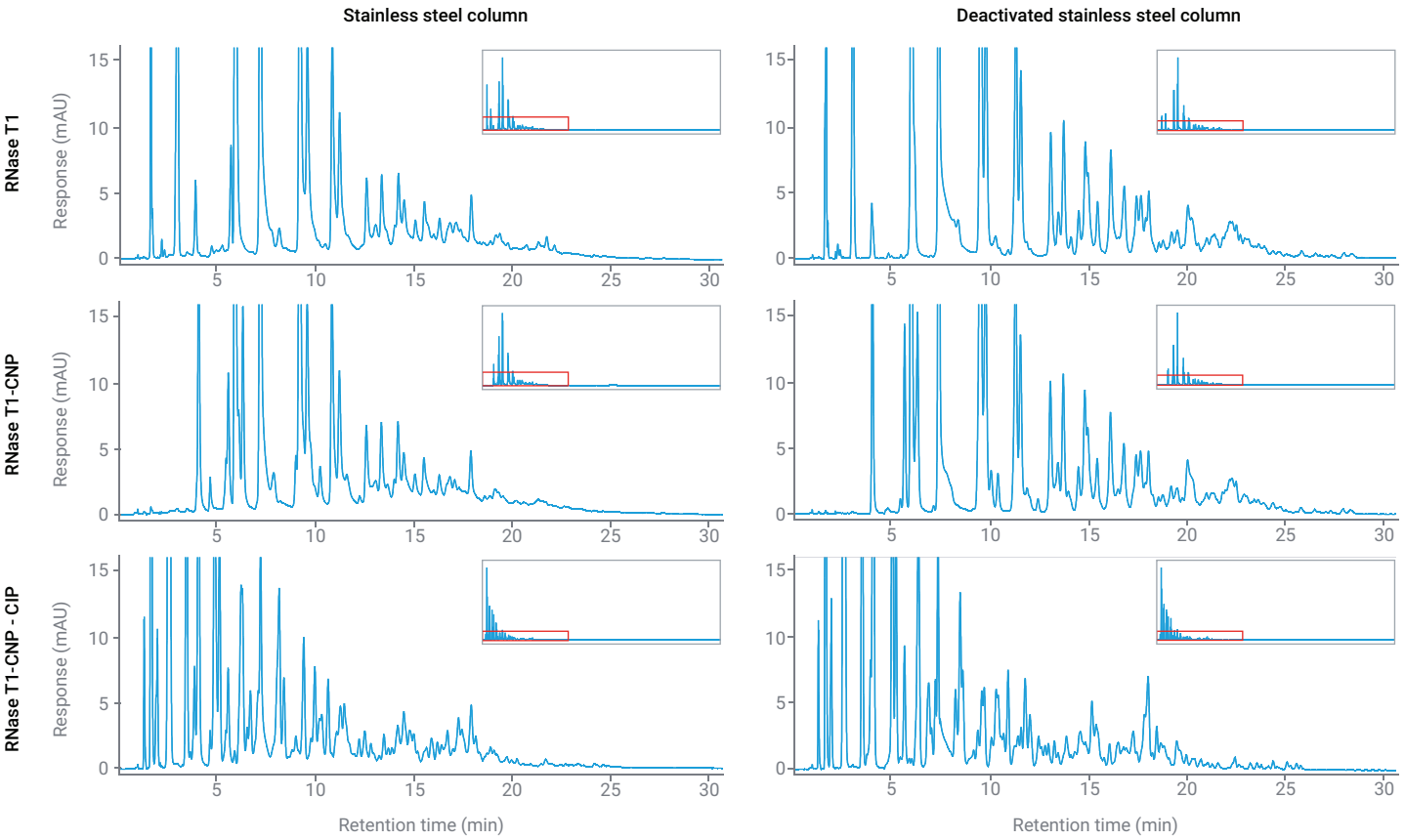

Figure 5. HILIC-UV chromatograms (260 nm) of Cas9 mRNA subjected to sequential digestion with RNase T1, CNP, and CIP, analyzed on a fully passivated conventional stainless-steel HILIC-Z column and a deactivated HILIC-Z column (LC Method 2).

Conclusion

HILIC has proven to be a viable and effective alternative to traditional IP-RPLC methods for the separation of oligonucleotides. As demonstrated in this application note, nonspecific adsorption of oligonucleotides to the iron surface of conventional stainless-steel columns represents significant challenges, including reduced detection sensitivity and pronounced peak tailing. It was demonstrated that the conventional stainless-steel HILIC-Z column required extensive conditioning to deliver repeatable performance, whereas the deactivated stainless-steel HILIC-Z column exhibited superior performance from the very first injection. Despite column passivation, the stainless-steel column could not fully match the deactivated stainless-steel column in terms of analyte recovery and peak shape. Furthermore, it was shown that peak tailing on the stainless-steel column could largely be attributed to the presence of linear 3'-phosphate termini on 5' RNA fragments, whereas 2',3'-cyclic phosphate termini contributed only minimally to nonspecific adsorption. These findings underscore the importance of selecting appropriate LC hardware and carefully considering the nature of terminal phosphate groups when employing HILIC for oligonucleotide separation in RNA mapping workflows.

References

1. Sahin, U.; Karikó, K.; Türeci, Ö. mRNA-Based Therapeutics—Developing a New Class of Drugs. *Nat. Rev. Drug Discov*. **2014**, *13(10)*, 759–780. https://doi.org/10.1038/nrd4278.
2. Maurer, J.; Vanluchene, H.; Tsalmpouris, A.; Morreel, K.; Camperi, J.; Sandra, K.; Guillarme, D. Exploring the Potential of Oligonucleotide Mapping with Liquid Chromatography–Mass Spectrometry to Study the Primary Structure of mRNA. *TrAC, Trends Anal. Chem.* **2025**, *191*, 118309. https://doi.org/10.1016/j.trac.2025.118309.
3. Lardeux, H.; D'Atri, V.; Guillarme, D. Recent Advances and Current Challenges in Hydrophilic Interaction Chromatography for the Analysis of Therapeutic Oligonucleotides. *TrAC, Trends Anal. Chem*. **2024**, *176*, 117758. https://doi.org/10.1016/j.trac.2024.117758.
4. Vanhoenacker, G.; Morreel, K.; Jonckheere, S.; Sandra, P.; Sandra, K.; Schneider, S.; Huber, U. Determining mRNA Capping with HILIC-MS on a Low-Adsorption Flow Path. *Agilent Technologies application note*, publication number 5994-7118EN, **2024**.
5. Vanluchene, H.; Morreel, K.; De Vos, J.; Sandra, P.; Sandra, K.; Schneider, S.; Huber, U. mRNA Mapping with IP-RPLC-MS on a Low-Adsorption Flow Path. *Agilent Technologies application note*, publication number 5994-8055EN, **2025**.
6. Bartlett, M. G. Current State of Hydrophilic Interaction Liquid Chromatography of Oligonucleotides. *J. Chromatogr. A* **2024**, *1736*, 465378. https://doi.org/10.1016/j.chroma.2024.465378.
7. Goyon, A.; Scott, B.; Kurita, K.; Crittenden, C. M.; Shaw, D.; Lin, A.; Yehl, P.; Zhang, K. Full Sequencing of CRISPR/Cas9 Single Guide RNA (sgRNA) via Parallel Ribonuclease Digestions and Hydrophilic Interaction Liquid Chromatography–High-Resolution Mass Spectrometry Analysis. *Anal. Chem.* **2021**, *93(44)*, 14792–14801. https://doi.org/10.1021/acs.analchem.1c03533.
8. Goyon, A.; Scott, B.; Yehl, P.; Zhang, K. Online Nucleotide Mapping of mRNAs. *Anal. Chem.* **2024**, *96(21)*, 8674–8681. https://doi.org/10.1021/acs.analchem.4c00873.
9. Wolf, E. J.; Grünberg, S.; Dai, N.; Chen, T. H.; Roy, B.; Yigit, E.; Corrêa, I. R., Jr. Human RNase 4 Improves mRNA Sequence Characterization by LC–MS/MS. *Nucleic Acids Res*. **2022**, *50(18)*, e106. https://doi.org/10.1093/nar/gkac632.

www.agilent.com

DE-010994

Printed in the USA, December 10, 2025
5994-8834EN

Agilent
Trusted Answers